Evaluation of remodeling process in small-diameter cell-free tissue-engineered arterial graft

Shuhei Tara, MD, PhD,[a] Hirotsugu Kurobe, MD, PhD,[a] Mark W. Maxfield, MD,[b] Kevin A. Rocco, MS,[b] Tai Yi, MD,[a] Yuji Naito, MD, PhD,[b] Christopher K. Breuer, MD,[a] and **Toshiharu Shinoka, MD, PhD,[a]**
Columbus, Ohio; and New Haven, Conn

Objective: **Autologous grafts are used to repair atherosclerotic cardiovascular diseases; however, many patients lack suitable donor graft tissue. Recently, tissue engineering techniques have emerged to make biologically active blood vessels. We applied this technique to produce arterial grafts using established biodegradable materials without cell seeding. The grafts were evaluated in vivo for vessel remodeling during 12 months.**
Methods: **Poly(L-lactide-co-ε-caprolactone) scaffolds reinforced by poly(lactic acid) (PLA) fiber were prepared as arterial grafts. Twenty-eight cell-free grafts were implanted as infrarenal aortic interposition grafts in 8-week-old female SCID/Bg mice. Serial ultrasound and micro computed tomography angiography were used to monitor grafts after implantation. Five grafts were harvested for histologic assessments and reverse transcription-quantitative polymerase chain reaction analysis at time points ranging from 4 months to 1 year after implantation.**
Results: **Micro computed tomography indicated that most implanted mice displayed aneurysmal changes (three of five mice at 4 months, four of five mice at 8 months, and two of five mice at 12 months). Histologic assessments demonstrated extensive tissue remodeling leading to the development of well-circumscribed neovessels with an endothelial inner lining, a neointima containing smooth muscle cells and elastin, and a collagen-rich extracellular matrix. There were a few observed calcified deposits, located around residual PLA fibers at 12 months after implantation. Macrophage infiltration into the scaffold, as evaluated by F4/80 immunohistochemical staining, remained after 12 months and was focused mostly around residual PLA fibers. Reverse transcription-quantitative polymerase chain reaction analysis revealed that gene expression of Itgam, a marker for macrophages, and of matrix metalloproteinase 9 was higher than in native aorta during the course of 12 months, indicating prolonged inflammation (Itgam at 8 months: 11.75 ± 0.99 vs native aorta, $P < .01$; matrix metalloproteinase 9 at 4 months: 4.35 ± 3.05 vs native aorta, $P < .05$).**
Conclusions: **In this study, we demonstrated well-organized neotissue of cell-free biodegradable arterial grafts. Although most grafts experienced aneurysmal change, such findings provide insight into the process of tissue-engineered vascular graft remodeling and should allow informed rational design of the next generation of arterial grafts. (J Vasc Surg 2014;■:1-10.)**

Clinical Relevance: **Tissue-engineered vascular grafts (TEVGs) hold promise for correcting some types of congenital heart disease because they are biocompatible, are antithrombogenic, and possess the capacity for growth. Recently, some studies showed the feasibility of TEVG for arterial graft using animal models. The aim of this study was to evaluate and to characterize the tissue remodeling process of one such TEVG made from clinically approved biodegradable materials. In this study, we report a highly patent TEVG featuring organized neotissue but that had some instances of aneurysmal change. These findings provide insight into the TEVG remodeling process and enable better design of next-generation arterial grafts.**

Atherosclerotic cardiovascular disease (CVD) is a systemic narrowing and hardening of the arteries and includes conditions such as coronary heart disease, carotid artery stenosis, and peripheral arterial disease. CVD affects millions of patients and is the leading cause of morbidity and mortality in the United States.[1] Surgical intervention using autologous arterial and venous grafts is the most common corrective procedure for CVD; however, many patients lack suitable donor tissue because of previous surgery or as a result of their underlying vascular disease. Alternative synthetic grafts, such as expanded polytetrafluoroethylene (Gore-Tex) and polyethylene terephthalate (Dacron), have a history of long-term success when they are placed in large arteries whose flow is high and resistance low. However, current synthetic small-diameter (<6 mm) grafts are prone to occlusion by thrombogenesis and as a result are contraindicated. Synthetic materials have several other drawbacks, including risk of infection, persistent inflammation, calcification, and chronic need for anticoagulant therapy.

To address these challenges, tissue engineering techniques have emerged to make biologically active blood

From the Tissue Engineering Program and Surgical Research, Nationwide Children's Hospital, Columbus[a]; and the Department of Surgery, Yale University School of Medicine, New Haven.[b]

Author conflict of interest: C.K.B. and T.S. receive grant support from Gunze Ltd and the Pall Corp; this funding was not used to support the work described in this manuscript. H.K. (in 2011) and S.T. (in 2012) were recipients of the Banyu Fellowship from Banyu Life Science Foundation International (Tokyo, Japan). H.K. (in 2013) was recipient of a fellowship from Shinsenkai Imabari Daiichi Hospital (Ehime, Japan).

Reprint requests: Toshiharu Shinoka, MD, PhD, 700 Children's Dr, Columbus, OH 43205 (e-mail: toshiharu.shinoka@nationwidechildrens.org).

The editors and reviewers of this article have no relevant financial relationships to disclose per the JVS policy that requires reviewers to decline review of any manuscript for which they may have a conflict of interest.
0741-5214/$36.00

http://dx.doi.org/10.1016/j.jvs.2014.03.011

vessels, called tissue-engineered vascular grafts (TEVGs). The traditional concept of tissue engineering consists of the following three components: (1) a tissue-inducing scaffold material, (2) the isolation and use of cells or cell substitutes, and (3) the integration of the cells and the scaffold by a seeding technique.[2] We have successfully applied this technique in a low-pressure environment (<30 mm Hg)[3] and have performed TEVG implantation in 25 pediatric patients in Japan.[4] Currently, we have begun a clinical trial in the United States with approval of the Food and Drug Administration (FDA) for implantation of TEVGs in patients undergoing extracardiac total cavopulmonary connection procedures. To achieve this, we employ highly porous, biodegradable grafts composed of poly(L-lactide-co-ε-caprolactone) (PLCL) reinforced by mesh of poly(glycolic acid) that are seeded with bone marrow-derived mononuclear cells. As the synthetic scaffolding degrades away, a new blood vessel is formed in its place by the infiltration of the host's own smooth muscle cells and endothelial cells from the adjacent native blood vessel.

For the TEVG strategy to be translated to arterial applications, the graft must withstand arterial pressures while maintaining sufficient porosity for cellular infiltration. Moving toward that reality, we confirmed the feasibility of TEVGs with and without cell seeding in a small-diameter arterial model.[5,6] Furthermore, several groups have also demonstrated different types of TEVGs without cell seeding for small-diameter arterial grafts.[7,8] The electrospinning technique, which enables the production of nanofiber-based scaffolds, has been proposed as a promising technique for fabrication of arterial TEVGs[9] and has shown good surgical and mechanical properties with a high patency rate in an arterial implantation model.[10] However, we believe that cellular migration into the scaffold was likely inhibited by the tightly knitted nanofiber, causing prolonged neotissue remodeling and foreign body reaction. Moving forward, we created a cell-free TEVG for arterial circulation constructed from PLCL and reinforced by poly(lactic acid) (PLA) fiber mesh (PLA-PLCL grafts) to enhance cell migration into the scaffold. Herein, we used the PLA-PLCL grafts to evaluate the process of vessel remodeling with implantation in a mouse abdominal aorta model during a 12-month period.

METHODS

Animals. All animals received humane care in compliance with the National Institutes of Health *Guide for the Care and Use of Laboratory Animals*. The Institutional Animal Care and Use Committee at Yale University approved the use of animals and all procedures described in this study. The 8-week old female SCID/Bg mice were purchased from Jackson Laboratories (Bar Harbor, Me).

Scaffolds. PLA-PLCL grafts were constructed with use of a dual-cylinder chamber molding system from a nonwoven 100% PLA fiber mesh (molecular weight, 120,000; Biomedical Structures, Warwick, RI) and a 50:50 PLCL (molecular weight, 360,000; Gunze Co, Ltd, Kyoto, Japan) sealant solution on the basis of conventional grafts previously described.[6] Pore size of the scaffold was about 30 μm, and wall thickness was about 250 μm. Wall thickness changed over time according to tissue remodeling. Each scaffold was 3 mm in length, and inner luminal diameters were between 500 and 600 μm (Fig 1, *A*). All scaffolds were sterilized by overnight ultraviolet radiation preceding implantation.

Graft implantation. Twenty-eight grafts were implanted as infrarenal aortic interposition conduits with a running 10-0 nylon suture for the end-to-end proximal and distal anastomoses by standard microsurgical technique (Fig 1, *B*). Details of the method for graft implantation were described in our previous report.[5] Neither antiplatelet nor anticoagulant agents were used during aortic cross-clamping or the perioperative period in this study. Because we observed an entirely equivalent model with the same graft for 6 weeks in our previous study,[6] we decided the time point for evaluation of late-term tissue remodeling to be 4, 8, and 12 months. Five mice were selected randomly and sacrificed at each time point, and harvested grafts were separated in half for different analysis.

Twelve sham operations were performed (opening and closing of the abdomen with exposure of the aorta) to evaluate the natural causes of aortic disease, such as aortic calcification and dilation, for 12 months.

Ultrasound. Serial ultrasonography (Vevo Visualsonics 770; Visualsonics, Toronto, Ontario, Canada) was used to serially monitor grafts after implantation. Before ultrasonography, mice were anesthetized with 1.5% inhaled isoflurane.

Contrast-enhanced micro computed tomography (CT) angiography. We selected five mice at each time point randomly, and in vivo micro CT angiography was performed under anesthesia with the GE eXplore Locus in vivo micro CT scanner (GE Healthcare, Milwaukee, Wisc). One minute before image acquisition, animals were given an intrajugular 0.3 mL bolus of Ultravist (370 mg I/mL; Bayer Healthcare, Wayne, NJ). Micro CT data were transferred to the Advanced Workstation (version 4.4; GE Healthcare) for further reconstruction and quantitative analysis. Measurements of graft length, inner luminal diameter, and graft volume were performed. Similar measurements were obtained in controls having undergone sham operation.

Histology and immunohistochemistry. Explanted grafts at 4, 8, and 12 months after implantation and native abdominal aortas were fixed in 4% paraformaldehyde and embedded in paraffin. Sections 5 μm thick were then stained by standardized techniques for hematoxylin and eosin, Masson trichrome, elastica-van Gieson, and von Kossa.

Identification of endothelial cells, smooth muscle cells, macrophages, and matrix metalloproteinase 2 (MMP-2) was done by immunohistochemical staining of paraffin-embedded explant sections with rabbit anti-CD31 (1:50; Abcam, Cambridge, Mass), mouse anti-smooth muscle actin (1:500; Dako, Carpinteria, Calif), rat anti-F4/80 (1:1000; AbD Serotec, Oxford, UK), and rabbit anti-MMP-2

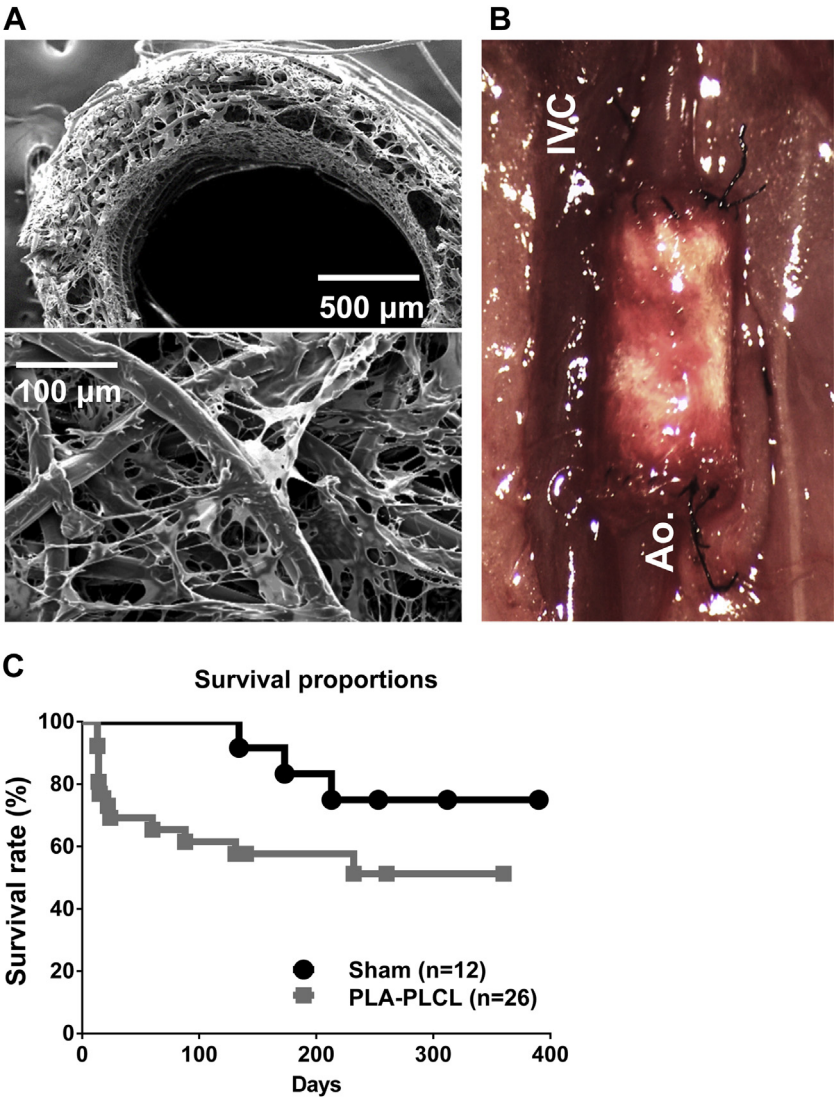

Fig 1. A, Scanning electron microscopy image of biodegradable scaffold, with porous microstructure allowing cellular infiltration. **B,** Intraoperative photograph demonstrating tissue-engineered vascular graft during surgical implantation. *Ao*, Aorta; *IVC*, inferior vena cava. **C,** Survival proportions during follow-up period of poly(lactic acid)-poly(L-lactide-co-ε-caprolactone) (*PLA-PLCL*) graft group compared with sham group.

(1:500; Abcam), respectively. Primary antibody binding was detected with biotinylated goat anti-rat immunoglobulin G (1:200; Vector, Burlingame, Calif), biotinylated goat anti-rabbit immunoglobulin G (1:200; Vector), and biotinylated goat anti-mouse immunoglobulin G (1:200; Vector), respectively. This was followed by the binding of streptavidin–horseradish peroxidase and color development with 3,3-diaminobenzidine.

RNA extraction and reverse transcription-quantitative polymerase chain reaction (RT-qPCR). Explanted grafts at 4, 8, and 12 months after implantation and native abdominal aortas were frozen in optimal cutting temperature (OCT) compound (Tissue-Tek; Sakura Finetek, Torrance, Calif) and sectioned into 20 sections of 30 μm with a Leica CM 1950 cryostat (Leica Biosystems, Wetzlar, Germany). Excess OCT compound was removed by centrifugation in phosphate-buffered saline. Total RNA was extracted and purified by the RNeasy Mini Kit (Qiagen, Venlo, The Netherlands) according to the manufacturer's instructions. Reverse transcription was performed with a High Capacity RNA-to-cDNA Kit (Applied Biosystems, Carlsbad, Calif). All reagents and instrumentation for gene expression analysis were obtained from Applied Biosystems. RT-qPCR was performed with a StepOnePlus Real-Time PCR System using the TaqMan Universal PCR Master Mix Kit. Reference numbers for primers are as follows: collagen type I (Cola1; Mm00801666_g1), collagen type III (Col3a1; Mm01254476_m1), elastin (Eln; Mm00514670_m1),

vimentin (vim; Mm01333430_m1), integrin alpha M (Itgam; Mm00434455_m1), matrix metallopeptidase 2 (MMP-2; Mm00439498_m1), matrix metallopeptidase 9 (MMP-9; Mm00442991_m1), transforming growth factor β1 (TGF-β1; Mm01178820_m1), and hypoxanthine-guanine phosphoribosyltransferase (HPRT; Mm00446968_m1). The results were analyzed with the comparative threshold cycle method and normalized with HPRT as an endogenous reference and reported as relative values (ΔΔ CT) to those of control native aorta.

Statistical analysis. To decide the sample number, a power calculation by log-rank test with .05 of α error and .8 of power was completed. We estimated that the event-free survival rate at the time point of 12 months after the implantation was 0.98 for the sham operation group and 0.3 for the PLA-PLCL implantation group. Results are expressed as mean ± standard deviation, and the number of experiments is shown in each case. Data for RT-qPCR were statistically analyzed by one-way analysis of variance followed by Tukey HSD. A probability value of less than .05 was considered statistically significant. All statistical analysis was done with SPSS (version 20; IBM, Armonk, NY).

RESULTS

Microsurgical implantation of tissue-engineered vascular grafts in mice as infrarenal interposition aortic conduits. Twenty-eight PLA-PLCL grafts were implanted as infrarenal interposition aortic conduits, and 12 syngeneic mice underwent sham operations. Perioperative survival was 92.9% in the PLA-PLCL graft group and 100% in the sham group. The survival rate of the remaining 26 mice in the PLA-PLCL graft group was 53.8% at 12 months (sham group, 75.0%) (Fig 1, *C*). Twelve mice from the PLA-PLCL graft group died of graft rupture, and three mice of the sham group died of undetermined causes. These were confirmed by autopsy within 24 hours after death.

Serial ultrasonographic imaging demonstrated luminal patency and laminar flow in all grafts through 12 months. Implanted grafts were serially monitored by ultrasound to assess for both patency and aneurysm. Doppler ultrasound detected normal blood flow at the proximal and distal ends of the implanted grafts and also within each graft (Fig 2, *A*). The images of implanted PLA-PLCL grafts with and without aneurysmal change are shown in Fig 2, *B*.

Assessment of graft morphometry by micro CT angiography demonstrated dilation to 12 months after implantation. In vivo micro CT angiography was performed at months 4 (n = 5), 8 (n = 5), and 12 (n = 5). Age-matched controls were also analyzed at each time point (n = 2-3 in each point). Most implanted mice had evidence of aortic dilation including aneurysmal change (three of five mice at 4 months, four of five mice at 8 months, and two of five mice at 12 months; Fig 2, *C*).

Luminal volume calculations with a standard graft length of 3 mm were as follows: native aorta, 0.8 ± 0.08 mm^3; PLA-PLCL graft, 2.3 ± 0.7 mm^3 at 4 months, 2.7 ± 0.6 mm^3 at 8 months, and 2.0 ± 0.8 mm^3 at 12 months (Fig 2, *D*).

Histologic assessment and RT-qPCR demonstrated cellular infiltration and neovessel remodeling. Histologic assessment demonstrated cell infiltration within the scaffolding as early as 4 months after implantation with a concomitant neointima (Fig 3, *A*). However, abundant PLA fibers, which may appear as vacuoles or capillaries, still existed in the scaffold layer at 12 months after implantation. Although the neointimal layer progressively augmented in thickness during the course of 12 months, the inner surface of this layer was covered by a confluent monolayer of endothelial cells (Fig 3, *B*).

Extracellular matrix (ECM) is the primary determinant of the biomechanical properties of neovessel. Consequently, we evaluated ECM components including collagen and elastin by histology and RT-qPCR. Although PLA fiber remained at 12 months, Masson trichrome staining showed a gradual increase in deposition of collagen within the polymer scaffolding (Fig 4, *A*). These qualitative assessments were quantitatively confirmed with gene expression by RT-qPCR. Collagen type I increased during the course of 12 months and collagen type III peaked at 8 months, and these levels were significantly higher than those of native aorta (collagen type I at 12 months: 4.69 ± 1.57 vs native aorta, $P < .001$; collagen type III at 8 months: 2.30 ± 0.38 vs native aorta, $P < .01$; Fig 4, *B*). Although elastin deposition within the neointimal layer was shown on elastica-van Gieson staining (Fig 4, *A*), gene expression of elastin in the PLA-PLCL graft was lower than that in native aorta (8 months: 0.33 ± 0.05 vs native aorta, $P < .05$; Fig 4, *B*).

Smooth muscle cells are the predominant cells in the arterial wall and are essential for the structural and functional integrity of the neovessel. In the present study, smooth muscle cells, which were defined by immunohistochemical smooth muscle actin staining, were shown at 8 months in the neointima and augmented at 12 months after implantation (Fig 4, *A*). Last, gene expression of vimentin, a mesenchymal cell marker, increased during the course of 12 months (12 months: 3.64 ± 0.86 vs native aorta, $P < .001$; Fig 4, *B*).

We were not able to collect data comparing the neotissue components between aneurysmal and nonaneurysmal grafts.

Macrophage infiltration and MMP activity in neotissue were elevated during the course of 12 months after implantation. Previously, we demonstrated that TEVGs transformed into functional neovessels by an inflammatory process of vascular remodeling,[11] and macrophages have been shown to play critical roles in this process.[12] MMPs degrade structural components within the ECM, and MMP-2 and MMP-9 were shown to be involved in the remodeling process of TEVGs.[13]

In this study, macrophage infiltration into scaffold, evaluated by F4/80 immunohistochemical staining, remained at 12 months, localized around the remaining

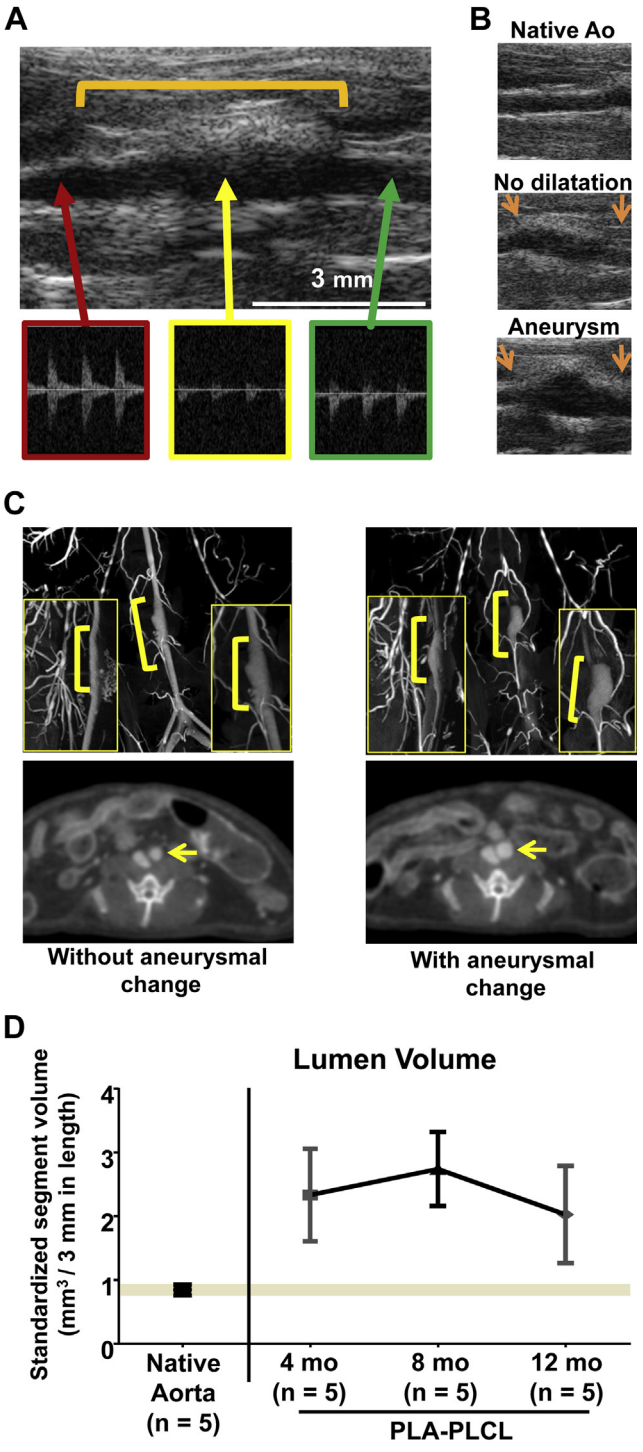

Fig 2. A, Serial Doppler ultrasound examinations were performed on poly(lactic acid)-poly(L-lactide-co-ε-caprolactone) (*PLA-PLCL*) grafts. All grafts remained patent to the experimental end point. **B,** Ultrasound images of no dilation and aneurysm of PLA-PLCL graft compared with native abdominal aorta (*Ao*). The *arrows* indicate the anastomoses. **C,** In vivo micro computed tomography (CT) angiography (n = 5/each time point) was performed at 4, 8, and 12 months. *Yellow bar* indicates approximate location of PLA-PLCL graft in a three-dimensional reconstructed micro CT image. The *arrows* in cross-sectional micro CT images indicate the implanted graft. **D,** Luminal volume was calculated by micro CT image processing software. Graft luminal volumes were standardized to a 3-mm segment.

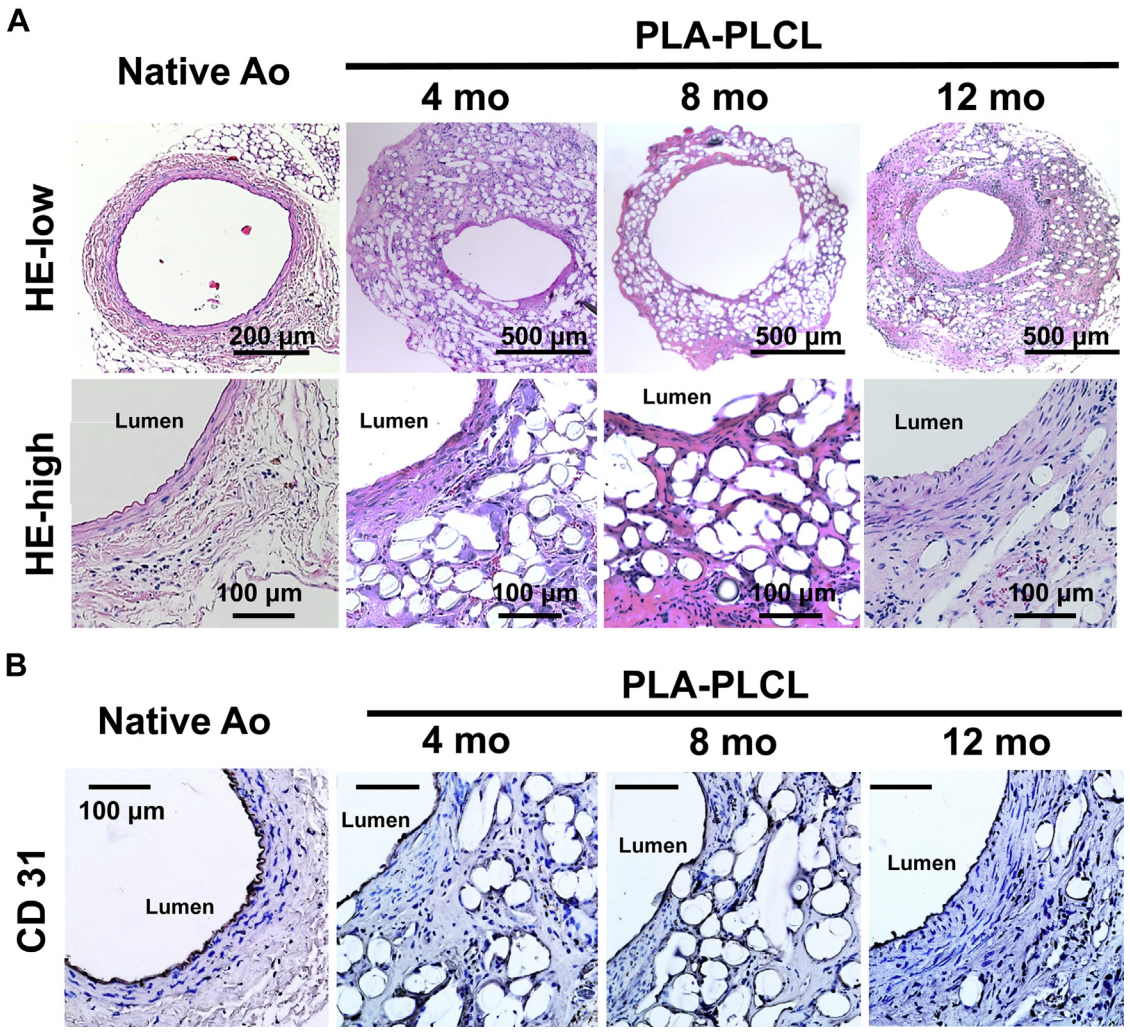

Fig 3. Representative histologic image of **(A)** hematoxylin and eosin (*HE*) staining with low- and high-power magnifications and **(B)** CD31 immunohistochemical staining. Grafts at 4, 8, and 12 months after implantation and native abdominal aortas were explanted, and formalin-fixed paraffin-embedded 5-μm cross sections were stained with HE or endothelial cell marker CD31 primary antibody at each time point and analyzed for cell infiltration and an endothelial layer, respectively. *Ao*, Aorta; *PLA-PLCL*, poly(lactic acid)-poly(L-lactide-co-ε-caprolactone).

PLA polymer fibers (Fig 5, *A*). Sustained elevation of MMP-2 activity was observed at each time point and exclusively at the interface between the graft layer and the intimal layer at 12 months (Fig 5, *A*). RT-qPCR analysis revealed that gene expression of Itgam for macrophage marker, MMP-2, and MMP-9 was higher than in native aorta (Itgam at 8 months: 11.75 ± 0.99 vs native aorta, $P < .01$; MMP-2 at 8 months: 2.68 ± 0.41 vs native aorta, $P < .05$; MMP-9 at 4 months: 4.35 ± 3.05 vs native aorta, $P < .05$; Fig 5, *B*).

TGF-β1 has been shown to play an important role in tissue repair as it is a key regulator of the production and remodeling of the ECM through its effect on mesenchymal cells.[14] For evaluation of the ongoing neovessel remodeling, the gene expression of TGF-β1 was measured and shown to be higher in TEVGs than in native aorta at each time point, indicating an active and ongoing remodeling process throughout the 12 months (12 months: 3.45 ± 0.52 vs native aorta, $P < .001$; Fig 5, *B*).

Calcific deposition in neotissue. During the course of neovessel remodeling, these implants are susceptible to calcification, a potentially fatal problem in a long-term application. von Kossa staining showed that there was no calcification in the neointimal layer at all during the course of 12 months, although a little calcification was observed around the remaining PLA fiber (Fig 5, *A*).

DISCUSSION

In this study, we used a mouse aortic implantation model with a cell-free PLCL scaffold reinforced by PLA

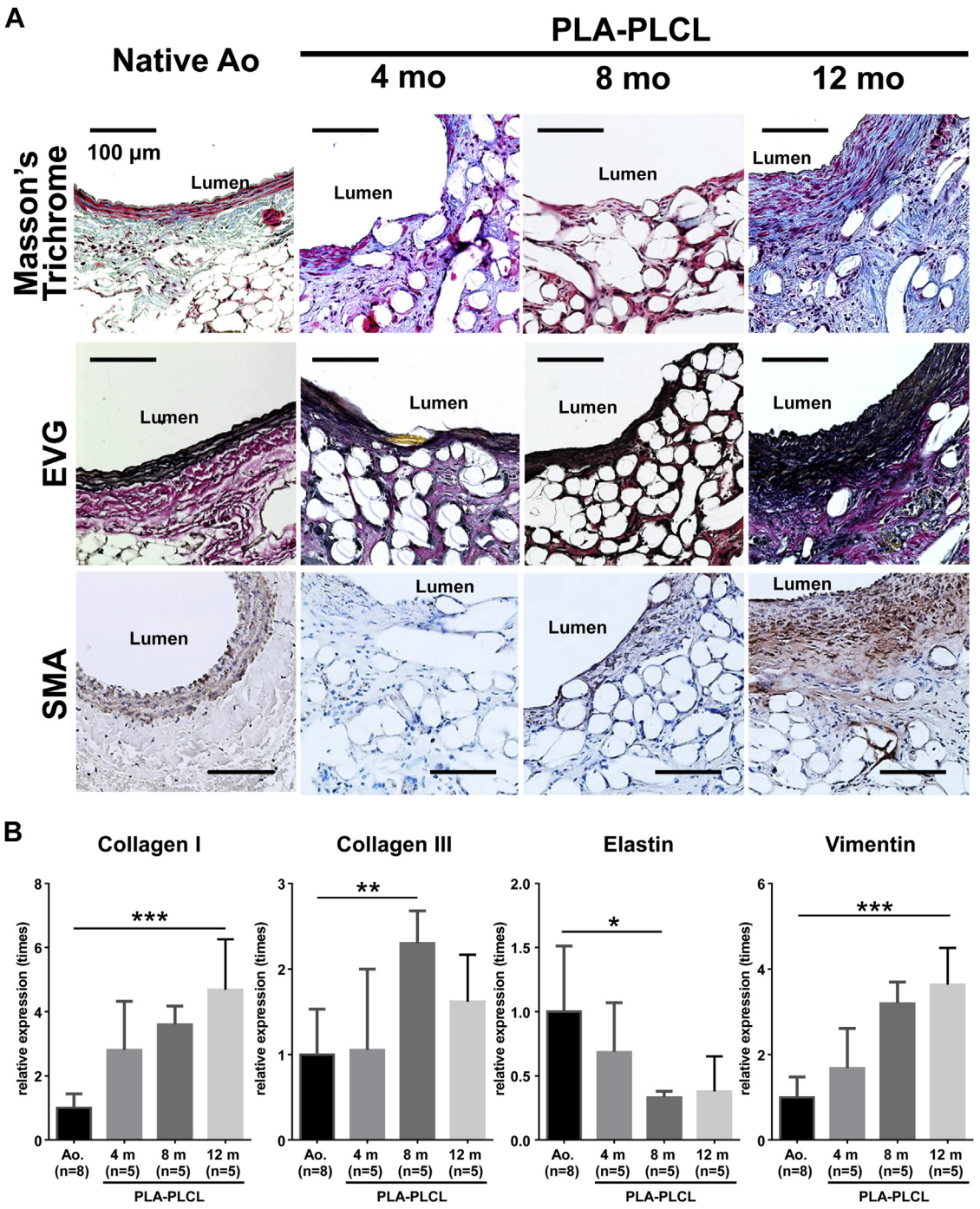

Fig 4. Neotissue formation of poly(lactic acid)-poly(L-lactide-co-ε-caprolactone) (*PLA-PLCL*) graft. Collagen and elastin deposition in neovessels was evaluated by histology and reverse transcription-quantitative polymerase chain reaction (RT-qPCR). **A,** Representative histologic image of Masson trichrome staining for collagen deposition, elastica-van Gieson (*EVG*) staining for elastic formation, and immunohistochemical smooth muscle actin (*SMA*) staining for smooth muscle cells within the neointima at 4, 8, and 12 months after implantation. *Ao*, Aorta. **B,** Gene expression of eight native aortas (control) and five grafts at each time point was analyzed by RT-qPCR with the ΔΔ CT method. Vimentin was used as a marker of mesenchymal cells including smooth muscle cells. Data are expressed as fold change over native aorta expression (mean ± standard deviation; $^{*}P < .05$, $^{**}P < .01$, $^{***}P < .001$).

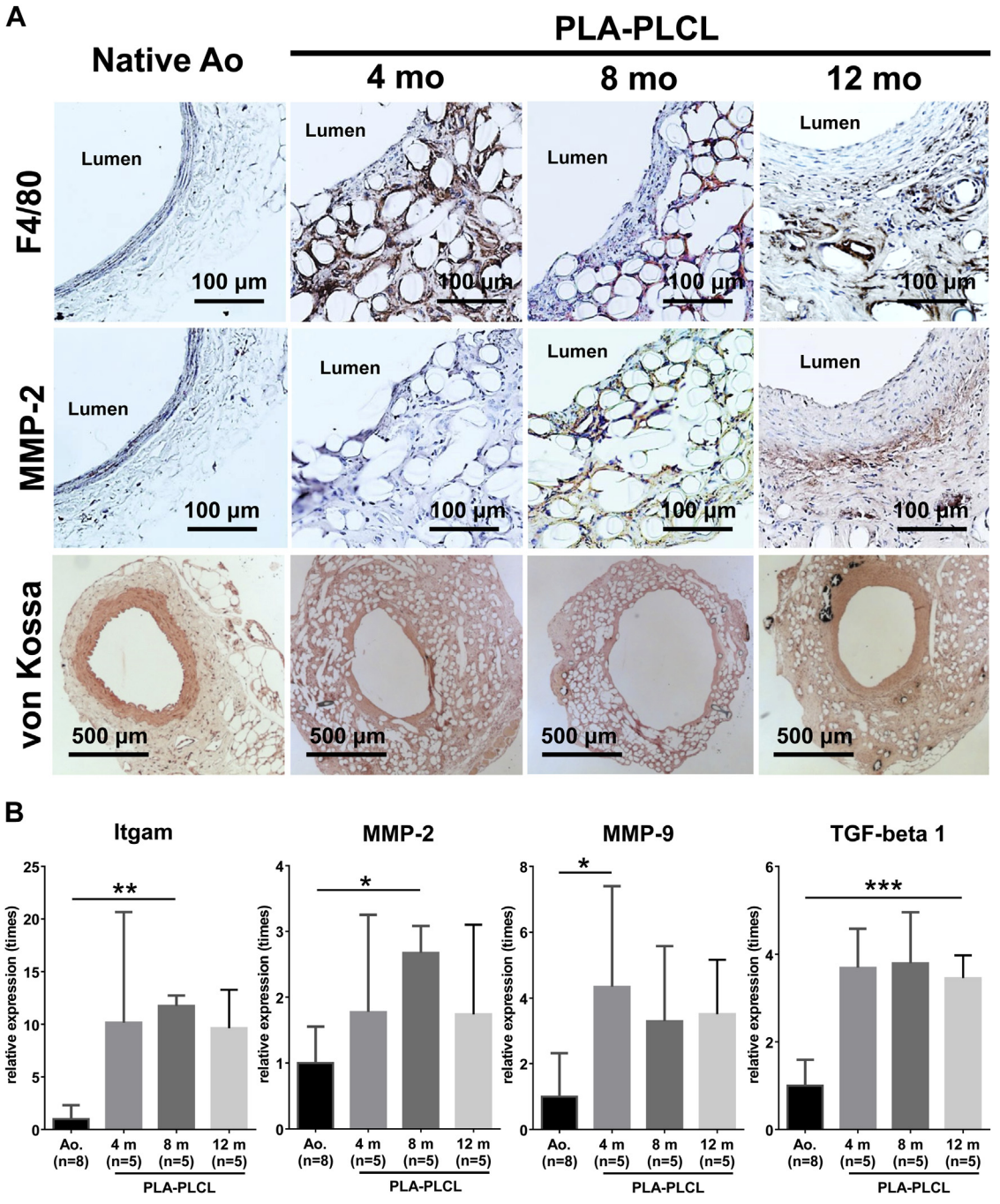

Fig 5. Inflammatory process and calcification of poly(lactic acid)-poly(L-lactide-co-ε-caprolactone) (*PLA-PLCL*) graft. Macrophage infiltration and matrix metalloproteinase (*MMP*) activity in neotissue were evaluated by immunohistochemical staining and reverse transcription-quantitative polymerase chain reaction (RT-qPCR). Calcification in neotissue was evaluated by von Kossa staining. **A,** Representative images of immunohistochemical stainings of macrophage marker F4/80 and MMP-2 and von Kossa staining at 4, 8, and 12 months after implantation. *Ao,* Aorta. **B,** Gene expression of eight native aortas (control) and five grafts at each time point was analyzed by RT-qPCR with the ΔΔ CT method. Itgam was used as a macrophage marker. Data are expressed as fold change over native aorta expression (mean ± standard deviation; $*P < .05$, $**P < .01$, $***P < .001$). *TGF,* Transforming growth factor.

fiber mesh as a biodegradable arterial TEVG. Advantages of the present investigation, compared with previous studies,[7-10] are that these materials are commonly used for constructing TEVGs because of their history of successful clinical application, are FDA approved for human implantation, and possess a broad range of material properties.[15] The construction of our graft in this study is comparable to the TEVG for inferior vena cava implantation that is already accepted for use in a clinical trial in the United States.[16] Furthermore, we observed this model for 12 months.

Neovessel formation is a dynamic process characterized by progressive degradation of the scaffold due to hydrolysis, cellular infiltration into the scaffold, and ECM deposition. The degradation period of our PLCL is approximately 4 to 6 weeks and that of PLA is more than 1 year.[6] The basic concept of our graft is to induce neovessel remodeling according to the degradation of PLCL while providing reinforcement by the PLA fiber mesh even after the disappearance of PLCL. Our study showed that 4 months after implantation, the PLCL was completely degraded with robust cellular infiltration, while PLA fibers still remained at 12 months. The neovessel demonstrated progressive remodeling, leading to the development of well-circumscribed tissue with an endothelial inner lining and a neointima containing collagens, elastin, and smooth muscle cells, although we did not collect data analyzing the function of these cells.

Whereas the present model of the arterial graft can achieve our basic TEVG strategy, most grafts experienced dilation or aneurysmal change from the first time point (4 months). Previously, we observed no aneurysm of the same arterial PLA-PLCL graft until 6 weeks after implantation.[6] These findings indicate that aneurysmal degeneration of PLA-PLCL began between 6 weeks and 4 months after implantation. The purported mechanism of aneurysmal degeneration of the graft is that neotissue formation in the scaffold was not enough to endure arterial pressure during the course of PLA degradation. Furthermore, continuous inflammation and MMP activity might be involved in this process. To solve this issue, TEVG design may require two approaches, including stronger reinforcement, such as combinational use of electrospinning,[7-10] and improvement of cellular growth and ECM deposition in the scaffold. Heparin coating on TEVGs has the potential to facilitate cell infiltration into the scaffold as well as to decrease the risk of thrombosis,[7] and other cytokines may improve remodeling of TEVGs. Techniques of local cytokine release from the scaffold are another option for TEVGs to achieve "off-the shelf" availability.

The gene expression of elastin in our graft remained lower than that in native aorta, although elastica-van Gieson staining suggested the presence of elastin in the neointima as early as 4 months after implantation. The elastic matrix is responsible for providing vessels with the necessary compliance for systolic stretch.[17] In the present study, the elastin observed by histology might be either insufficient or less functional, considering our results that most of the implants displayed aneurysmal changes. The protein product of the elastin gene is synthesized by vascular smooth muscle cells and secreted as a tropoelastin monomer,[18] and its deposition was enhanced when stimulated by cyclic stretching.[19,20] In the present study, we speculate that mechanical stimulation of the smooth muscle cells by pulsatile stretching may have been limited by the residual PLA fibers, thereby reducing elastin production or function in the neoartery.

Histologic assessments indicated that macrophage infiltration into scaffold peaked at an early phase of neotissue formation, and smooth muscle cells were present 8 months after implantation. MMP activity was assessed by gene expression of MMP-9 and MMP-2. We found that MMP-9 expression peaked in the earlier phase of neovessel formation relative to that of MMP-2. MMP-9 is known as the most prominent type of MMP present in a foreign body inflammatory response,[21] and macrophage infiltration is promoted by MMP-9.[22] Consecutively, the migration of smooth muscle cells was shown to be dependent on MMP-2 and MMP-9.[22] MMP-2 is mainly produced by mesenchymal cells when stimulated by inflammatory cells.[23] In our previous study using a cell-seeded TEVG implanted into the mouse inferior vena cava, MMP-9 peaked at 1 week after implantation and decreased thereafter, although MMP-2 increased during the 4-week observation period.[13] These findings indicate that the process of foreign body reaction and tissue remodeling in the present arterial model is similar to our previous venous model but probably prolonged because of the remaining PLA fiber.

The results of this study showed that gene expression of TGF-β1 was higher than that of native aorta during the course of the observation period. TGF-β is a multifunctional cytokine that regulates cell proliferation, differentiation, adhesion, migration, and apoptosis.[24] TGF-β signaling plays an essential role in vascular remodeling, and its abnormality is known to cause vascular dysfunction such as aortic aneurysm.[24] Our previous study indicated that the PLA-PLCL graft possessed sufficient mechanical strength and properties to function as an arterial graft after testing of burst pressure, suture retention strength, Young modulus, and tensile strength and demonstrated no aneurysmal formation after short-term (6-week) follow-up.[6] On the basis of these findings, continuous elevation of TGF-β at later time points might induce the vascular dysfunction of our grafts followed by aneurysmal change. Interestingly, angiotensin receptor blockers are known to inhibit TGF-β signaling and to prevent aortic aneurysm in Marfan syndrome.[25,26] This drug may also have therapeutic potential to prevent aneurysmal change of the arterial TEVG in our model.

At the beginning of this study, we predicted thrombosis or occlusion of our PLA-PLCL graft with high frequency at the time point of 12 months because our previous short-term observation using wild-type C57BL/6 mice showed a high-frequency rate of these events. However, our present finding did not support this initial

hypothesis. One possible reason is that the SCID/Bg model may prevent thrombosis and neotissue hyperplasia of the PLA-PLCL graft. On the basis of this limitation, we have created an aortic implantation model in the wild-type C57BL/6 mouse without acute thrombosis by use of antiplatelet and anticoagulant drugs. Furthermore, vascular dysfunction followed by aneurysm may be caused even after complete scaffold degradation. Therefore, we must evaluate vascular function of arterial TEVGs with a model of long-term follow-up, such as in large animals.

CONCLUSIONS

We observed a cell-free PLA-PLCL graft for 12 months in a mouse aortic implantation model. Although well-organized neotissue was demonstrated, aneurysmal rupture was observed in 46% of implanted TEVGs. The concept of a cell-free arterial TEVG was partially proven in an arterial system with use of FDA-approval materials.

We acknowledge the excellent technical assistance of Cameron A. Best, Paul S. Bagi, and Zhen W. Zhuang. We would also like to thank Nancy Troiano, Rose Webb, and Christiane Coady of the Yale Core Center for Musculoskeletal Disorders for their technical expertise in processing murine TEVG tissue.

AUTHOR CONTRIBUTIONS

Conception and design: ST, HK, TS
Analysis and interpretation: ST, HK, MM, KR, TY, YN
Data collection: ST, HK, MM, KR, TY, YN
Writing the article: ST, HK
Critical revision of the article: ST, HK, CB, TS
Final approval of the article: ST, HK, MM, KR, TY, YN, CB, TS
Statistical analysis: ST, HK
Obtained funding: CB, TS
Overall responsibility: TS
ST and HK contributed equally to this article and share co-first authorship.

REFERENCES

1. Lim LS, Haq N, Mahmood S, Hoeksema L. Atherosclerotic cardiovascular disease screening in adults: American College Of Preventive Medicine position statement on preventive practice. Am J Prev Med 2011;40:381.e1-e10.
2. Langer R, Vacanti JP. Tissue engineering. Science 1993;260:920-6.
3. Shin'oka T, Imai Y, Ikada Y. Transplantation of a tissue-engineered pulmonary artery. N Engl J Med 2001;344:532-3.
4. Hibino N, McGillicuddy E, Matsumura G, Ichihara Y, Naito Y, Breuer C, et al. Late-term results of tissue-engineered vascular grafts in humans. J Thorac Cardiovasc Surg 2010;139:431-6.
5. Mirensky TL, Nelson GN, Brennan MP, Roh JD, Hibino N, Yi T, et al. Tissue-engineered arterial grafts: long-term results after implantation in a small animal model. J Pediatr Surg 2009;44:1127-32.
6. Roh JD, Nelson GN, Brennan MP, Mirensky TL, Yi T, Hazlett TF, et al. Small-diameter biodegradable scaffolds for functional vascular tissue engineering in the mouse model. Biomaterials 2008;29:1454-63.
7. Wu W, Allen RA, Wang Y. Fast-degrading elastomer enables rapid remodeling of a cell-free synthetic graft into a neoartery. Nat Med 2012;18:1148-53.
8. Kuwabara F, Narita Y, Yamawaki-Ogata A, Satake M, Kaneko H, Oshima H, et al. Long-term results of tissue-engineered small-caliber vascular grafts in a rat carotid arterial replacement model. J Artif Organs 2012;15:399-405.
9. Mrowczynski W, Mugnai D, de Valence S, Tille JC, Khabiri E, Cikirikcioglu M, et al. Porcine carotid artery replacement with biodegradable electrospun poly-e-caprolactone vascular prosthesis. J Vasc Surg 2014;59:210-9.
10. Wang S, Mo XM, Jiang BJ, Gao CJ, Wang HS, Zhuang YG, et al. Fabrication of small-diameter vascular scaffolds by heparin-bonded P(LLA-CL) composite nanofibers to improve graft patency. Int J Nanomedicine 2013;8:2131-9.
11. Roh JD, Sawh-Martinez R, Brennan MP, Jay SM, Devine L, Rao DA, et al. Tissue-engineered vascular grafts transform into mature blood vessels via an inflammation-mediated process of vascular remodeling. Proc Natl Acad Sci U S A 2010;107:4669-74.
12. Hibino N, Yi T, Duncan DR, Rathore A, Dean E, Naito Y, et al. A critical role for macrophages in neovessel formation and the development of stenosis in tissue-engineered vascular grafts. FASEB J 2011;25:4253-63.
13. Naito Y, Williams-Fritze M, Duncan DR, Church SN, Hibino N, Madri JA, et al. Characterization of the natural history of extracellular matrix production in tissue-engineered vascular grafts during neovessel formation. Cells Tissues Organs 2012;195:60-72.
14. Klass BR, Grobbelaar AO, Rolfe KJ. Transforming growth factor beta1 signalling, wound healing and repair: a multifunctional cytokine with clinical implications for wound repair, a delicate balance. Postgrad Med J 2009;85:9-14.
15. Athanasiou KA, Niederauer GG, Agrawal CM. Sterilization, toxicity, biocompatibility and clinical applications of polylactic acid/polyglycolic acid copolymers. Biomaterials 1996;17:93-102.
16. Shinoka T, Breuer C. Tissue-engineered blood vessels in pediatric cardiac surgery. Yale J Biol Med 2008;81:161-6.
17. Venkataraman L, Ramamurthi A. Induced elastic matrix deposition within three-dimensional collagen scaffolds. Tissue Eng Part A 2011;17:2879-89.
18. Patel A, Fine B, Sandig M, Mequanint K. Elastin biosynthesis: the missing link in tissue-engineered blood vessels. Cardiovasc Res 2006;71:40-9.
19. Kolpakov V, Rekhter MD, Gordon D, Wang WH, Kulik TJ. Effect of mechanical forces on growth and matrix protein synthesis in the in vitro pulmonary artery. Analysis of the role of individual cell types. Circ Res 1995;77:823-31.
20. Seliktar D, Nerem RM, Galis ZS. Mechanical strain-stimulated remodeling of tissue-engineered blood vessel constructs. Tissue Eng 2003;9:657-66.
21. Jones JA, McNally AK, Chang DT, Qin LA, Meyerson H, Colton E, et al. Matrix metalloproteinases and their inhibitors in the foreign body reaction on biomaterials. J Biomed Mater Res A 2008;84:158-66.
22. Hu J, Van den Steen PE, Sang QX, Opdenakker G. Matrix metalloproteinase inhibitors as therapy for inflammatory and vascular diseases. Nat Rev Drug Discov 2007;6:480-98.
23. Davis V, Persidskaia R, Baca-Regen L, Itoh Y, Nagase H, Persidsky Y, et al. Matrix metalloproteinase-2 production and its binding to the matrix are increased in abdominal aortic aneurysms. Arterioscler Thromb Vasc Biol 1998;18:1625-33.
24. Goumans MJ, Liu Z, ten Dijke P. TGF-beta signaling in vascular biology and dysfunction. Cell Res 2009;19:116-27.
25. Habashi JP, Judge DP, Holm TM, Cohn RD, Loeys BL, Cooper TK, et al. Losartan, an AT1 antagonist, prevents aortic aneurysm in a mouse model of Marfan syndrome. Science 2006;312:117-21.
26. Brooke BS, Habashi JP, Judge DP, Patel N, Loeys B, Dietz HC 3rd. Angiotensin II blockade and aortic-root dilation in Marfan's syndrome. N Engl J Med 2008;358:2787-95.

Submitted Jan 9, 2014; accepted Mar 7, 2014.